Published in final edited form as:
Nature. 2017 September 27; 549(7673): 507–510. doi:10.1038/nature23645.

Earth's volatile contents established by melting and vaporisation

C. Ashley Norris and **Bernard J. Wood**
Department of Earth Sciences, University of Oxford, South Parks Road, Oxford OX1 3AN, U.K.

Abstract

The silicate Earth is strongly depleted in moderately volatile elements (e.g. Pb, Zn, In, alkalis) relative to CI chondrites, the meteorites which compositionally most closely resemble the Sun1. Qualitatively the depletion "trend" may be explained by accretion of 10-20% of a volatile-rich body to a reduced volatile-free protoEarth2,3 followed by partial extraction of some elements to the core1. Several issues remain, however, notably the overabundance of In in silicate Earth which leads to questions about the sources of Earth's volatiles4,5. Here we have examined the melting processes which attended accretion on Earth and precursor bodies and performed vaporisation experiments under conditions of fixed temperature and oxygen partial pressure. We find that the pattern of volatile element depletion in silicate Earth is consistent with partial melting and vaporisation rather than with simple accretion of a volatile-rich chondrite-like body. We argue that melting and vaporisation on precursor bodies and possibly during the giant moon-forming impact6–8 was responsible for establishing the observed abundances of moderately volatile elements in the Earth.

The Earth accreted from asteroidal and protoplanetary bodies over a timescale of 30-100 M.yr9. Based on observations of igneous, metallic and achondritic meteorites, many of these asteroidal components formed within a few M.yr of the origin of the solar system and underwent an early phase of melting and vaporisation, with heat sources such as the decay of 26Al9. Volatile-poor Vesta, for example appears to have formed within 4 Ma of the origin of the solar system and to have undergone melting, volatile loss10 and volcanism for a further 35 M.yr11. During the Earth's protracted accretion unmelted and previously melted, variably volatile-depleted bodies were added in impacts which became progressively more violent, terminating with the giant impact (or impacts) which led to the Moon6,12. Modelling of the accretion process and applying constraints based on the partitioning of siderophile elements between core and silicate mantle leads to the conclusion that the Earth was periodically covered by a "magma ocean" of molten silicate13–15. Models of the giant

Author contributions
AN constructed the furnace, performed the experiments and analyses and contributed to writing the manuscript. BW conceived the project, provided guidance and wrote a substantial part of the manuscript.

Competing Financial Interests
The authors declare that they have no competing financial interests.

Data Availability
The authors declare that all data supporting the findings of this study are available within the paper and its supporting and extended data files.

Europe PMC Funders Author Manuscripts

impact also suggest that this led to wholesale melting of the silicate Earth, extremely high surface temperatures with partial vaporisation of the silicate melt12,16 and generation of a proto-lunar disk of melt and vapour. Some volatile loss can take place from this proto-lunar disk by hydrodynamic escape17. Atmospheric loss from the Earth during the magma ocean phase18 and loss of moderately volatile Zn8,19 and K7 from the Moon is confirmed by recent isotopic measurements.

As anticipated from the previous discussion, the silicate Earth is strongly depleted in moderately volatile elements such as Pb, Tl, Zn, Sb, Bi and Ag relative to the solar composition as represented by CI chondrites. Figure 1 illustrates these depletions in a graph of element concentration in silicate Earth1 normalised to abundance in CI chondrites plotted against a measure of element volatility. The latter is assumed, following general practise, to correlate with the temperature at which 50% of the element would be condensed from a gas of solar composition 20. For comparison we show the depletion pattern of CV carbonaceous chondrites21, meteorites which are also volatile- depleted relative to CI chondrites and which have never undergone planetary processes of melting and core formation.

From Figure 1 it can be seen that, although there is a general trend of declining relative abundance in both the silicate Earth and in CV chondrites with increasing volatility (decreasing condensation temperature) there are many elements which, in silicate Earth, fall below the trend. Such cases are frequently ascribed to extraction into the core, either in segregating Fe-rich metal22 during accretion or in a putative sulfide “Hadean matte” in the final stages of core formation2. Thus, for example, elements such as Au, Cu, Ag, and S are known to partition strongly into both molten Fe metal22 and liquid FeS at elevated temperature while the more abundant Na, K, B, and F, show negligible tendencies to follow them into the core. Core formation has clearly reduced the concentrations of relatively involatile elements such as Fe, Ni, Mo and W, in silicate Earth23 so it is reasonable to apply the same principle to the volatile elements of Figure 1. Implicitly, however, this approach to understanding the chemical composition of silicate Earth relies on the assumption that the moderately volatile elements were added to Earth during accretion by a body of 10-20% of Earth’s mass which had CI chondrite-like ratios of these elements. Late arrival of such a body appears to be the most reasonable explanation of the Pd/Ag and $^{107}Ag/^{109}Ag$ ratios of silicate Earth3. This body has also been suggested to have been the moon-forming impactor2. Further depletions as shown for Au, Ag and other elements are then ascribed to the core-forming processes mentioned above1. Despite the flexibility of the approach in terms of conditions (pressure, temperature, metal composition) of core formation, however, which can be varied to match the depletion pattern, the abundances of numerous elements remain difficult to explain. Indium, for example, has a much lower condensation temperature than Zn and is more siderophile and more chalcophile than Zn22 yet is relatively more abundant in silicate Earth1. In is also much more abundant in silicate Earth than Tl despite having similar condensation temperature (Figure 1) and being both more siderophile and more chalcophile than Tl22. Cs is strongly depleted despite not partitioning significantly into either metal or sulfide24. The same applies to the halogens. Cu and Ag have virtually identical partitioning into sulfide and metal22 and very similar condensation temperatures, yet Cu is substantially more abundant than Ag. The pattern of abundance of Figure 1 cannot, it appears, be explained solely by addition of volatiles in a CI-like body followed by partial

core formation. Of the other processes involved in the formation and differentiation of the Earth, melting on precursor bodies and on the protoplanet must have led to partial vaporisation of the most volatile elements and it is this process which we consider here.

In order to directly measure the loss of volatile elements to the vapour phase a one–atmosphere gas mixing furnace with stirring apparatus was constructed (see methods and extended data). This device was capable of stirring a 4.5cm^3 crucible of silicate melt at temperatures up to 1700°C in an entirely gas-tight assembly. Flowing CO/CO_2 mixtures were used to control oxygen fugacity. The crucible and stirrer mechanism were made of high-purity nickel and products were drop-quenched into a water bath at the end of the experiment. The silicate starting material was a natural basalt from the Reykjanes Ridge, south of Iceland, crushed and ground and mixed with a trace element mixture of oxide powders designed to yield concentrations of 300-500μg.g^{-1} per element.

Volatile loss experiments were performed at 1300°C and a range of log(fO_2) values from −7 to −13. This fO_2 range represents values from just below the Ni-NiO buffer, characteristic of the modern mantle25 down to a value 2.3 log units below the Fe-FeO buffer. The latter value corresponds to the case of molten peridotitic mantle in equilibrium with Fe and hence simulates conditions during core formation.

All products presented as a mass of homogeneous black glass containing no observable gas bubbles.

Major element compositions of the products were determined by scanning electron microscope with Energy Dispersive detector (Extended Data Table 1). Trace element concentrations were measured by LA-ICP-MS (methods and Extended Data Table 2). Samples were inspected for homogeneity using an SEM with BSE imaging, X-Ray mapping, and repeated spot analysis by EDS. In all cases the major element composition of the samples appeared to be homogeneous to the precision of these techniques (~ 2% RSD).

Repeated trace element analysis by LA-ICP-MS showed that most elements are homogeneous to better than the single spot precision, approximately 5-10% RSD. At the high concentration range of 400-500 μg.g^{-1} the intra-spot variation is less than 5% RSD for elements Ag, Ga, In, Mo, Pb, Sn, W, and Zn. Those elements in the range 10-15% RSD are Bi, Cd, Cu, Ge, Sb, and Tl. Unsurprisingly, the most-depleted samples at an abundance of 1-10 μg.g^{-1} show more intra-spot variation as well as greater uncertainty for each point. The most variable elements are Bi, Ge, and Sb, with 25% RSD, then Ag, Cd, Sn, and Zn in the range 10-15% RSD, with the rest showing less than 10% RSD.

Over the duration of the experiment volatile elements partitioned into the gas phase and were flushed from the furnace by the constant stream of CO/CO_2 gas. For these volatile loss experiments the surface of the melt is continuously replenished by the stirring mechanism and diffusion of the element in the melt can be neglected as a kinetic factor.

Figure 2 shows a time series of experiments performed at fO_2 of 10^{-7} atm (0.3 logfO_2 units below the Ni-NiO buffer). As can be seen, loss is continuous with time and under these conditions, in contrast to condensation (Figure 1) Indium is less volatile than Cu or Ag. In

order to compare volatile loss from the silicate melt for each element we define a “volatility factor” (F_M) of trace element M to be the final concentration of the trace element divided by the initial concentration in the starting mixture. Low values correspond to high volatility. In order to determine the relative element volatilities and their dependence on oxygen fugacity it was necessary to select a constant experiment time at which volatility factors were compared. This must be a time at which most elements show some volatility and the volatility order is unchanging with time. It must not be so long that some of the elements of interest are no longer detectable by our analytical method. From figure 2 it is clear that the correct volatility order is established in 10-30 minutes and that some elements are almost completely lost after 3 hours, even at the relatively oxidising log fO_2 of -7. Given these constraints we opted to compare volatility factors after 60 minutes. This was simply a convenient time and was not chosen with any particular hypothesis in mind. All volatility factors in Figure 3 therefore refer to experiments of 60 minutes duration.

The volatility factors of trace elements are plotted against oxygen fugacity in Figure 3. There is a clear increase in volatility of elements with decreasing oxygen fugacity indicating that the gas species are more reduced than the oxide species in the melt.

In young solar systems the nebular H_2-rich gas is believed to disperse after about 3 Ma26 meaning that, thereafter, the conditions of melting induced by radioactive decay and impacts are set by the solid silicate and metal components equilibrated within the planetary or protoplanetary body. In the case of the Earth, Mars and Vesta, the oxygen fugacity imposed by core-mantle equilibrium would be in the range 1-3 log units below Fe-FeO equilibrium14,27. This means that oxygen fugacities of 10^{-11} to 10^{-13} atm would at 1300°C be appropriate for the estimation of volatilities from molten or partially molten silicate bodies undergoing core formation. Under these conditions, as shown in Figure 3, indium is less volatile than Cu, Zn, Pb, and Ag, all elements which have higher condensation temperatures (Figure 1). The principal reason for this is that solar gases have high concentrations of H_2S and H_2O and In has stable gaseous S and OH species (InS, In_2S, InOH) which stabilise it in the gas phase. These species are absent from our experiments. The latter, nevertheless provide a clue to the origin of the indium “anomaly”. This is readily explained if the moderately volatile element contents of silicate Earth were established by liquid-gas reaction during melting after the disappearance of the nebular gas. This might reasonably have been established on small precursor bodies for which gravitational escape would have been possible or conceivably during the Moon-forming impact when instabilities in the silicate vapour may have induced significant loss of the Earth-moon atmosphere17.

In Figure 4 we plot silicate Earth abundances of the elements we have studied against volatility factors under conditions of 1300°C and log fO_2 of -13 and -11. As can be seen, the pattern of depletion agrees closely with the volatility factors we have measured under conditions appropriate for core formation on precursor bodies and Earth. In detail, In, Cu, and Zn all have similar volatilities, consistent with their similar relative abundances in silicate Earth while Sn is more volatile and Cd, Ag, and Ge much more volatile than Zn, also consistent with their relative abundances. The plateau in abundances on the left hand side of Figures 4a and 4b is at a level close to 1%, which implies that the concentrations have been augmented by a chondritic component believed to have delivered 2 ± 1% of Earth’s C, H and

some noble gases28 and/or the “late veneer” which delivered ~0.5% of Earth’s highly siderophile elements after core formation ceased29.

In conclusion, we have shown that the pattern of volatile element abundance in silicate Earth (Figure 4) is much more consistent with measured volatilities from silicate melt at low fO_2 than with volatilities (condensation temperatures) in a solar gas (Figure 1). The data strongly suggest that the pattern of volatile element depletion was established by melt-vapour equilibrium (evaporation and re-condensation) in the absence of the reducing nebular gas. One can envisage this process most likely taking place on small molten precursor bodies where gravitational escape of volatiles is likely, or possibly from the Earth-moon system following the giant impact.

Methods

In order to directly measure the loss of volatile elements to the vapour phase a one–atmosphere gas mixing furnace with stirring apparatus was constructed. This device was capable of stirring a 4.5cm^3 crucible of silicate melt at temperatures up to 1700°C. Previous workers30 have built *in situ* stirring mechanisms integrated into gas-mixing furnaces, but our design features an entirely gas-tight assembly as well as a rapid-quenching mechanism. The furnace tube was made from high-purity alumina with heating elements of molybdenum disilicide. The crucible and stirrer mechanism were made of high-purity nickel. The purity of the nickel was verified by LA-ICP-MS (see analysis description below) to contain <3μg.g^{-1} of the trace elements of interest, except for Cu which was slightly elevated at 30μg.g^{-1} but still well below the concentration in the sample. Experiments were quenched in a water bath upon conclusion.

The starting material was made from natural basalt dredged from Reykjanes Ridge, south of Iceland, crushed in a Fritsch steel-jaw rock crusher before being ground to a fine grey powder using a Tema agate disc mill. To ensure a sufficient supply of material approximately 500g of material was crushed. A trace element mixture was formulated to target final compositions of 300-500μg.g^{-1} per element, weighed out from reagent-grade oxide powders. The trace element mixture was ground with a quarter of the powdered basalt in an agate mortar. The remainder of the basalt was added in 3 stages and ground together with the initial mixtures in a large agate mortar. In total 60 g of the starting material was prepared and stored in a desiccator to maintain dryness.

To determine the trace element composition of the starting mixture a portion of sample was melted and quenched to a glass in a high pressure piston cylinder experiment. This was run at 1.5GPa, 1500°C in a graphite capsule for 5 minutes. The product was mounted in acrylic, ground and polished with diamond paste prior to analysis by EDS and LA-ICP-MS (see below for analytical method). The composition of the starting mixture is shown in extended data Tables 1 and 2.

Volatile loss experiments were performed at 1300°C and a range of log fO_2 values from −7 to −13. The oxygen fugacity of the experiments was controlled using a constant CO/CO_2 gas mixture, apportioned according to the tables in Deines *et al.* 31. Verification of the oxygen

fugacity was performed before and after each experiment using a solid zirconia potentiometric oxygen sensor.

For each experiment, 3g of material was weighed out, pressed into a 12mm diameter pellet with a 10 ton press and placed inside the crucible. The crucible is keyed into the top of an alumina pedestal, which is inserted into the hot furnace from below. A second key between the pedestal and the base of the furnace ensures the crucible resists the turning moment from the stirrer. The assembly takes 1-2 minutes to come to temperature, with the sample melting around 1250°C. The stirrer was inserted from above, penetrating the molten sample by approximately 8 mm, and the furnace sealed. The stirrer was driven with a DC motor via a PWM motor controller. At 20% output power the stirrer would rotate constantly at 30 RPM. All experiments used the same stirring rate.

At the end of the experiment the stirrer was stopped and a trapdoor in the bottom of the furnace opened, allowing the pedestal and assembly to fall freely into a water bath.

All experiments presented as a mass of homogenous black glass containing no observable gas bubbles. Most samples filled at least half of the 4.5 mm^2 crucible, with a small amount of material fracturing and breaking free into the water bath. Analysis of any loose shards showed the same composition as the primary mass of sample. The samples were mounted in acrylic resin, ground, and polished with diamond paste prior to analysis.

Analysis

Samples were imaged using an FEI Quanta FEG 650 SEM and analysed using on Oxford X–MaxN standard-less EDS from Oxford Instruments mounted on the same instrument. Analysis was performed at 20kV with a focussed spot (< 1μm diameter) and 3nA beam current, measured by an absorbed current meter attached to the sample stage. All standard-less analyses of these basaltic glass samples were checked for accuracy against the secondary glass standards GSE−1G, GSD−1G, and GSC−1G 32,33 and MPI Ding basaltic glasses prior to each analytical session.

All experiments showed major element compositions (see extended data Table 1) that were uniform to within the precision of the analysis. In all samples the only change in major element composition was a variation in nickel concentration of the melt, ranging from 0.2 to 2.56% NiO. If the nickel content is removed and the remaining fraction normalised to 100% then the composition remains unchanged.

Trace element analysis was performed by LA–ICP–MS with a 213nm Nd:YAG laser (New Wave Research) and “large format” cell connected to a Perkin Elmer NexION 400Q ICP. The ICP was tuned for stability, minimal mass bias (U/Th ≈ 1.1 on SRM NIST610) and oxide production (ThO/Th < 0.2%) with a typical nebulizer gas flow of 450 $mL.min^{-1}$ and constant helium flow of 800 $mL.min^{-1}$. The USGS basaltic glass standard GSE-1G was used as a primary calibration standard, with ^{43}Ca as the internal standard, standard-sample bracketing, and data reduction by *Glitter*34. The laser was fired at 5 Hz with a 50 μm round spot, 4 $J.cm^{-2}$ of on-sample fluence, and scanned at 3 $\mu m.s^{-1}$ over 180 μm for 60s of signal. Between samples the cell was allowed to washout for 120s. A 20s gas blank was collected

prior to each ablation, and standards were sampled every 45 minutes. The following isotopes were measured for quantification of each element: ^{107}Ag, ^{209}Bi, ^{111}Cd, ^{53}Cr, ^{65}Cu, ^{71}Ga, ^{74}Ge, ^{115}In, ^{95}Mo, ^{208}Pb, ^{121}Sb, ^{118}Sn, ^{203}Tl, ^{51}V, ^{182}W, ^{66}Zn. A small (< 0.1%) overlap correction was applied for ^{115}Sn on ^{115}In. The detection limit for most elements was below 0.1 μg.g^{-1} which was more than adequate for quantification of these samples, with all concentrations (see extended data Table 2) well above detection.

To assess variations in the trace element composition of the melt the laser was scanned at random locations scattered across the exposed surface of the glass. All of the results show excellent trace element homogeneity. In the experiments performed at more reducing conditions, nickel blebs formed in the glass and were inadvertently sampled by the laser. Any signals from nickel blebs were discarded in the analysis.

Laser tracks were ablated perpendicular to the accessible surface of the glass. With a 40 μm spot it was possible to detect quantitative changes in the trace element composition. At this spatial resolution there was no observable change in the composition of any trace element at the surface of the melt, indicating that the stirring mechanism worked as designed and provided a continuous turnover of material throughout the experiment.

As well as nickel migrating into the melt, the nickel capsule absorbed small amount sof some trace elements. To assess the magnitude of this loss a number of LA–ICP–MS scans were performed from the glass into the neighbouring crucible. These scans show a small diffusion profile for some elements (Ag, Bi, Cu, In, and Sb), extending up to a maximum distance of 200 μm into the crucible. The effect of this diffusion would be to artificially enhance the perceived volatile loss of those elements. An attempt has been made to quantify this effect, and our assessment is that a worst-case 200 μm “rind” of enriched material on the inside of the crucible can equate to no more than 5% of the total volume of the melt. As such, diffusion into the capsule material can be neglected in these experiments.

Results

Over the duration of each experiment volatile elements partition into the gas phase and are flushed from the furnace by the constant stream of CO and CO_2 gas. Due to the stirring mechanism the surface of the melt is continuously replenished and diffusion of the element in the melt can be neglected. The longer the duration of the experiment the more of each element that is lost to the vapour phase. As shown in Figure 2, the relative degrees of volatile loss do not change with time. To quantitatively assess the volatile loss, the volatility factor is defined as the concentration at the end of the experiment divided by the starting concentration. In this study the 60 minute duration was chosen to achieve measurable depletion for the entire range of elements. Experiments were performed at a range of time durations at log fO_2 of -7, and at 60 minutes for log fO_2 of -9, -11, and -13. The compositions of each experiment are shown in Extended data Tables 1 and 2.

Extended Data

Europe PMC Funders Author Manuscripts

Extended Data Table 1

Major element compositions (weight %) of starting material (EBT1) and product glasses from experiments F006 to F019. 1σ refers to 1 standard deviation and N to the number of analyses.

Experiment	Mix	Duration (min)	Temperature (°C)	log(fO2)	N	SiO2	(σ)	TiO2	(σ)	Al2O3	(σ)	FeO	(σ)	MnO	(σ)
Starting	EBT1	0	N/A	N/A	5	50.66	0.04	0.96	0.02	15.11	0.02	9.69	0.08	0.20	0.02
F006	EBT1	10	1300	-7	10	50.70	0.04	0.98	0.02	15.22	0.03	9.41	0.06	0.22	0.03
F007	EBT1	30	1300	-7	10	50.50	0.05	0.97	0.02	15.20	0.03	9.33	0.03	0.24	0.02
F008	EBT1	60	1300	-7	11	50.33	0.32	1.01	0.02	15.05	0.04	9.54	0.07	0.26	0.02
F010	EBT1	180	1300	-7	10	49.82	0.06	0.99	0.02	14.87	0.04	8.82	0.12	0.37	0.01
F012	EBT1	5	1300	-9	10	50.73	0.08	0.98	0.02	15.27	0.03	9.51	0.18	0.23	0.02
F013	EBT1	30	1300	-9	10	50.59	0.19	0.98	0.02	15.19	0.05	9.34	0.04	0.24	0.02
F014	EBT1	60	1300	-9	10	50.64	0.08	0.98	0.02	15.26	0.03	8.99	0.10	0.29	0.03
F015	EBT1	30	1300	-11	10	50.82	0.18	0.96	0.01	15.39	0.10	9.00	0.08	0.24	0.04
F018	EBT1	60	1300	-11	10	50.30	0.09	0.99	0.02	15.11	0.03	9.21	0.06	0.23	0.03
F019	EBT1	60	1300	-13	10	50.87	0.14	0.98	0.02	15.14	0.03	9.02	0.08	0.24	0.02

Experiment	Mix	Duration (min)	Temperature (°C)	log(fO2)	N	MgO	(σ)	CaO	(σ)	Na2O	(σ)	K2O	(σ)	NiO	(σ)	Total	Total (σ)
Starting	EBT1	0	N/A	N/A	5	8.90	0.05	12.28	0.04	1.96	0.06	0.07	0.01	0	0	99.8	0.5
F006	EBT1	10	1300	-7	10	8.66	0.02	12.27	0.03	1.83	0.02	0.13	0.01	0.58	0.02	100.0	0.5
F007	EBT1	30	1300	-7	10	8.69	0.03	12.19	0.03	1.88	0.02	0.12	0.01	0.88	0.02	100.0	0.3
F008	EBT1	60	1300	-7	11	8.51	0.15	12.46	0.10	1.70	0.21	0.11	0.01	1.05	0.03	100.0	0.6
F010	EBT1	180	1300	-7	10	8.40	0.04	12.34	0.04	1.71	0.03	0.12	0.01	2.56	0.09	100.0	0.3
F012	EBT1	5	1300	-9	10	8.76	0.04	12.31	0.05	1.90	0.02	0.13	0.02	0.21	0.09	100.0	1.2
F013	EBT1	30	1300	-9	10	8.56	0.12	12.32	0.04	1.74	0.14	0.14	0.01	0.90	0.02	100.0	0.5
F014	EBT1	60	1300	-9	10	8.75	0.03	12.28	0.05	1.88	0.03	0.10	0.02	0.84	0.03	100.0	0.5
F015	EBT1	30	1300	-11	10	8.72	0.14	12.16	0.05	1.93	0.03	0.10	0.02	0.68	0.26	100.0	1.2
F018	EBT1	60	1300	-11	10	8.57	0.07	12.19	0.05	1.74	0.06	0.10	0.02	1.56	0.03	100.0	0.6
F019	EBT1	60	1300	-13	10	8.73	0.05	12.31	0.03	1.95	0.04	0.08	0.02	0.69	0.11	100.0	0.8

Europe PMC Funders Author Manuscripts

Extended Data Table 2

Trace element concentrations (ppm) and standard deviations (σ) of starting material and product glasses based on N analyses.

Experiment	N	Ag	(σ)	Bi	(σ)	Cd	(σ)	Cr	(σ)	Cu	(σ)	Ga	(σ)	Ge	(σ)	In	(σ)
Starting	41	328.6	10.1	203.1	17.1	355.0	43.4	600.6	88.4	309.6	22.9	315.1	92.7	446.2	122.1	378.4	40.0
F006	103	303.3	45.9	107.2	14.1	157.5	36.0	490.7	57.0	287.7	31.6	417.8	15.3	240.6	25.9	337.4	11.2
F007	134	223.9	54.0	49.7	21.3	91.1	41.7	542.8	60.3	243.5	48.6	416.5	14.9	146.2	51.3	304.0	17.7
F008	101	210.2	37.7	45.8	15.7	80.0	17.5	607.4	57.9	189.7	17.2	453.9	19.3	139.1	11.9	305.8	15.0
F010	38	13.7	1.2	2.3	0.3	0.8	0.1	711.7	28.0	31.6	3.4	439.2	21.0	11.1	3.6	186.8	7.6
F012	31	295.7	9.2	47.9	4.3	90.0	3.9	443.0	14.1	336.8	10.8	377.9	40.7	146.4	23.9	382.6	11.5
F013	31	247.3	16.7	71.5	18.6	133.9	11.5	574.6	22.6	257.2	16.2	427.8	10.5	226.6	13.6	307.7	10.6
F014	31	64.9	5.0	34.3	15.4	25.0	4.0	712.6	20.0	102.0	5.4	381.7	14.7	74.7	8.5	234.2	13.1
F015	30	163.1	60.9	72.7	30.5	96.0	25.7	590.6	48.9	192.0	62.5	354.5	107.9	189.0	41.0	238.4	23.1
F018	31	41.4	2.1	14.9	0.8	6.6	0.6	595.3	18.3	113.0	3.8	411.4	11.5	20.1	1.9	233.4	7.3
F019	63	7.1	6.2	1.7	1.4	6.6	2.9	700.6	120.1	54.3	42.5	210.0	102.1	6.2	1.6	72.2	53.1

Experiment	N	Mo	(σ)	Pb	(σ)	Sb	(σ)	Sn	(σ)	Tl	(σ)	V	(σ)	W	(σ)	Zn	(σ)
Starting	41	394.5	40.3	454.0	20.1	482.6	17.3	333.7	6.7	413.4	13.2	692.6	76.6	321.6	51.5	535.4	12.8
F006	103	477.1	13.3	485.0	23.4	332.7	30.2	215.7	10.5	260.7	17.9	802.5	25.7	709.8	28.3	553.8	22.9
F007	134	483.9	15.1	443.9	71.5	224.2	85.9	164.7	25.2	186.3	50.3	810.4	18.2	728.2	25.2	514.2	55.1
F008	101	492.3	25.0	463.4	33.2	218.4	39.6	155.7	9.8	215.2	20.2	836.7	29.1	799.3	34.9	550.7	34.3
F010	38	579.6	26.4	153.5	18.4	11.7	6.8	57.8	6.5	27.0	3.6	949.3	24.4	987.3	32.1	314.2	23.4
F012	31	474.2	27.0	890.1	36.1	253.0	33.5	110.3	12.4	357.9	8.2	741.9	44.6	452.0	52.8	754.0	37.1
F013	31	509.2	17.4	478.0	20.2	305.3	32.5	166.3	8.2	276.9	11.7	860.4	20.0	778.4	23.1	606.0	31.6
F014	31	458.4	14.0	291.9	28.4	101.0	34.1	64.5	5.5	163.2	15.5	844.8	20.6	750.9	24.1	328.6	27.3
F015	30	441.0	113.2	426.4	54.8	206.3	94.5	112.9	11.1	236.7	62.6	788.0	255.4	793.2	69.1	454.2	49.8
F018	31	442.9	12.2	164.5	6.8	5.7	0.4	66.6	2.8	51.4	2.1	811.1	20.9	710.2	25.5	259.4	9.3
F019	63	245.2	134.8	52.7	44.9	1.1	0.5	12.8	11.5	28.6	23.4	767.6	16.4	633.0	81.1	69.2	46.3

Europe PMC Funders Author Manuscripts

Acknowledgements

This research was supported by grants from the European Research Council (267764) and Science and Technology Facilities Council (UK) to BJW and a Studentship to AN from the STFC. We thank Don Dingwell and his group in Munich for advice on furnace design, Godfrey Fitton (Edinburgh) for donating the basalt we used and 3 anonymous referees for their constructive criticism.

References

1. Palme, H, O'Neill, H. Treatise on geochemistry volume 3. Vol. Ch. 1. Elsevier; 2014. 1–39.
2. O'Neill HS. The Origin of the Moon and the Early History of the Earth - a Chemical-Model .2. The Earth. Geochimica et Cosmochimica Acta. 1991; 55:1159–1172. DOI: 10.1016/0016-7037(91)90169-6
3. Schönbächler M, Carlson RW, Horan MF, Mock TD, Hauri EH. Heterogeneous accretion and the moderately volatile element budget of Earth. Science. 2010; 328:884–887. [PubMed: 20466929]
4. Wang ZC, Laurenz V, Petitgirard S, Becker H. Earth's moderately volatile element composition may not be chondritic: Evidence from In, Cd and Zn. Earth and Planetary Science Letters. 2016; 435:136–146. DOI: 10.1016/j.epsl.2015.12.012
5. Witt-Eickschen G, Palme H, O'Neill HSC, Allen CM. The geochemistry of the volatile trace elements As, Cd, Ga, In and Sn in the Earth's mantle: New evidence from in situ analyses of mantle xenoliths. Geochimica et Cosmochimica Acta. 2009; 73:1755–1778. DOI: 10.1016/J.Gca.2008.12.013
6. Canup RM, Asphaug E. Origin of the Moon in a giant impact near the end of the Earth's formation. Nature. 2001; 412:708–712. [PubMed: 11507633]
7. Wang K, Jacobsen SB. Potassium isotopic evidence for a high-energy giant impact origin of the Moon. Nature. 2016; 538:487–+. DOI: 10.1038/nature19341 [PubMed: 27617635]
8. Paniello RC, Day JMD, Moynier F. Zinc isotopic evidence for the origin of the Moon. Nature. 2012; 490:376–+. DOI: 10.1038/nature11507 [PubMed: 23075987]
9. Kleine T, et al. Hf-W chronology of the accretion and early evolution of asteroids and terrestrial planets. Geochimica et Cosmochimica Acta. 2009; 73:5150–5188. DOI: 10.1016/j.gca.2008.11.047
10. Moynier F, et al. Planetary-Scale Strontium Isotopic Heterogeneity and the Age of Volatile Depletion of Early Solar System Materials. Astrophys J. 2012; 758doi: 10.1088/0004-637x/758/1/45
11. Roszjar J, et al. Prolonged magmatism on 4 Vesta inferred from Hf-W analyses of eucrite zircon. Earth and Planetary Science Letters. 2016; 452:216–226. DOI: 10.1016/j.epsl.2016.07.025
12. Cuk M, Hamilton DP, Lock SJ, Stewart ST. Tidal evolution of the Moon from a high-obliquity, high - angular - momentum Earth. Nature. 2016; 539:402–406. DOI: 10.1038/nature19846 [PubMed: 27799656]
13. Li J, Agee CB. Geochemistry of mantle-core differentiation at high pressure. Nature. 1996; 381:686–689.
14. Wade J, Wood BJ. Core formation and the oxidation state of the Earth. Earth And Planetary Science Letters. 2005; 236:78–95.
15. Rubie DC, et al. Accretion and differentiation of the terrestrial planets with implications for the compositions of early-formed Solar System bodies and accretion of water. Icarus. 2015; 248:89–108. DOI: 10.1016/j.icarus.2014.10.015
16. Canup RM. Simulations of a late lunar-forming impact. Icarus. 2004; 168:433–456.
17. Genda H, Abe Y. Modification of a proto-lunar disk by hydrodynamic escape of silicate vapor. Earth Planets Space. 2003; 55:53–57.
18. Tucker JM, Mukhopadhyay S. Evidence for multiple magma ocean outgassing and atmospheric loss episodes from mantle noble gases. Earth and Planetary Science Letters. 2014; 393:254–265. DOI: 10.1016/j.epsl.2014.02.050
19. Kato C, Moynier F, Valdes MC, Dhaliwal JK, Day JMD. Extensive volatile loss during formation and differentiation of the Moon. Nat Commun. 2015; 6doi: 10.1038/Ncomms8617

20. Lodders K. Solar system abundances and condensation temperatures of the elements. Astrophys J. 2003; 591:1220–1247.
21. Wasson JT, Kallemeyn GW. Compositions of chondrites. Philosophical Transactions Royal Society London A. 1988; 325:535–544.
22. Wood BJ, Kiseeva ES, Mirolo FJ. Accretion and core formation: The effects of sulfur on metal-silicate partition coefficients. Geochimica et Cosmochimica Acta. 2014; 145:248–267. DOI: 10.1016/j.gca.2014.09.002
23. McDonough WF, Sun S-s. The composition of the Earth. Chemical Geology. 1995; 120:223–253.
24. Mills NM, Agee CB, Draper DS. Metal-silicate partitioning of cesium: Implications for core formation. Geochimica et Cosmochimica Acta. 2007; 71:4066–4081. DOI: 10.1016/j.gca.2007.05.024
25. Wood BJ, Bryndzia LT, Johnson KE. Mantle oxidation state and its relationship to tectonic environment and fluid speciation. Science. 1990; 248:337–345. [PubMed: 17784487]
26. Evans NJ, et al. The Spitzer c2d Legacy Results: Star-Formation Rates and Efficiencies; Evolution and Lifetimes. Astrophys J Suppl S. 2009; 181:321–350. DOI: 10.1088/0067-0049/181/2/321
27. Righter K, Drake MJ. Core Formation in Earth's Moon, Mars, and Vesta. Icarus. 1996; 124:513–529.
28. Marty B. The origins and concentrations of water, carbon, nitrogen and noble gases on Earth. Earth and Planetary Science Letters. 2012; 313-314:56–66.
29. Wang ZC, Becker H. Ratios of S, Se and Te in the silicate Earth require a volatile-rich late veneer. Nature. 2013; 499:328–+. DOI: 10.1038/Nature12285 [PubMed: 23868263]
30. Dingwell DB, O'Neill HSC, Ertel W, Spettel B. The solubility and oxidation-state of nickel in silicate melt at low-oxygen fugacities-Results using a mechanically assisted equilibration technique. Geochim Cosmochim Acta. 1994; 58:1967–1974.
31. Deines P, Nafziger RH, Ulmer GC, Woermann E. Temperature-Oxygen Fugacity Tables for Selected Gas-Mixtures in System C-H-O at One Atmosphere Total Pressure. Metall Trans B. 1976; 7:143–143. DOI: 10.1007/Bf02664703
32. Jochum KP, et al. MPI-DING glasses: New geological reference materials for in situ Pb isotope analysis. Geochem Geophy Geosy. 2005; 6doi: 10.1029/2005gc000995
33. Jochum KP, et al. GeoReM: A new geochemical database for reference materials and isotopic standards. Geostand Geoanal Res. 2005; 29:333–338. DOI: 10.1111/J.1751-908x.2005.Tb00904.X
34. Griffin W, Powell W, Pearson N, O'reilly S. GLITTER: data reduction software for laser ablation ICP-MS. Laser Ablation-ICP-MS in the earth sciences. Mineralogical association of Canada short course series. 2008; 40:204–207.

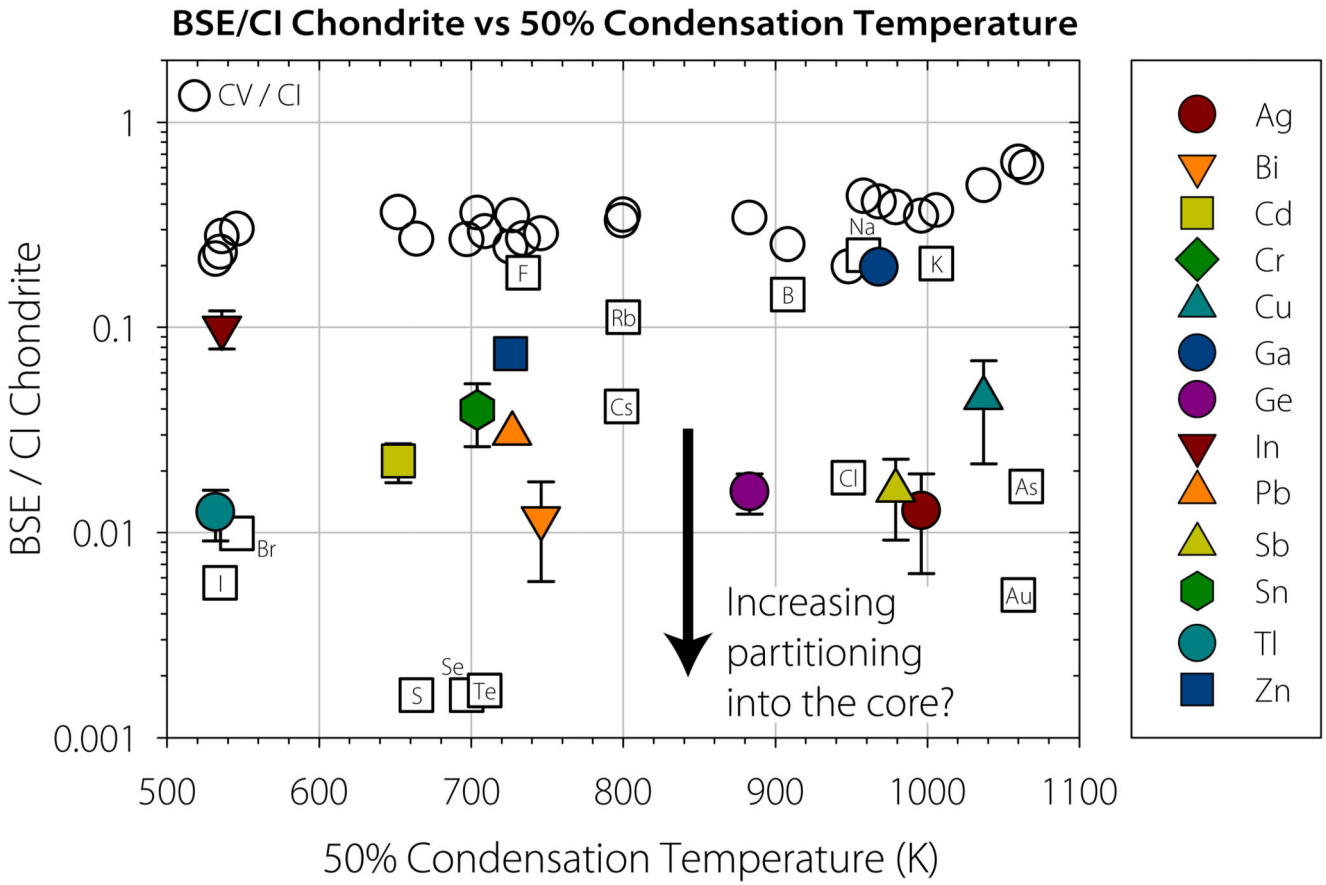

Figure 1.

Concentrations in Bulk Silicate Earth (BSE) of moderately volatile elements plotted versus their condensation temperatures from a gas of solar system composition16. Concentrations are expressed relative to concentrations in CI chondrite meteorites1 (normalised to a concentration ratio of Mg of 1.0). Elements studied here are shown in the key. Open squares refer to elements not specifically addressed by our study. Open circles refer to all elements in CV chondrites. Error bars are 1SD.

Europe PMC Funders Author Manuscripts

Europe PMC Funders Author Manuscripts

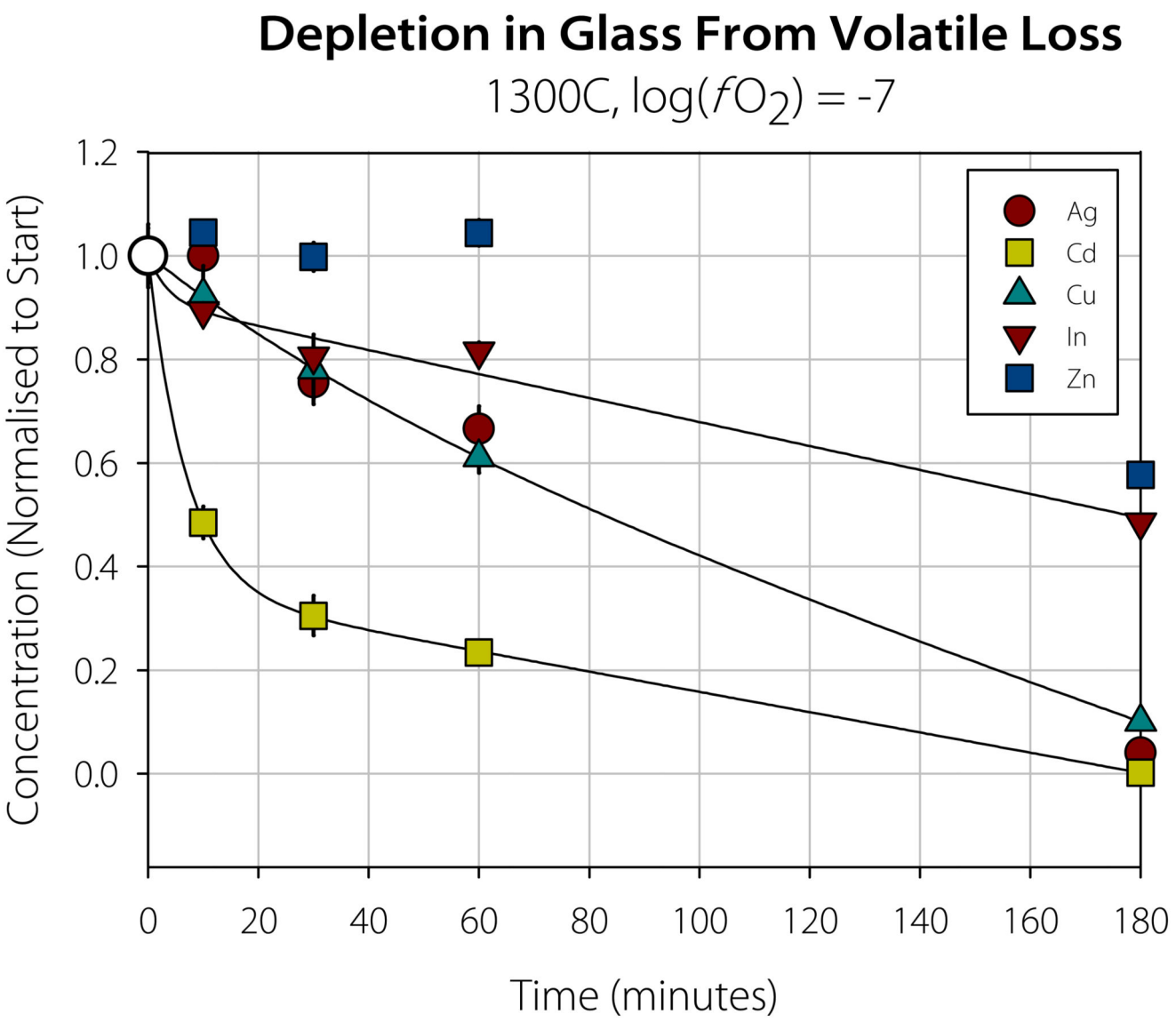

Figure 2.

Concentrations of selected elements in product silicate glasses, normalised to starting concentrations, for a time series performed at 1300°C and an oxygen fugacity of 10^{-7} atm. This oxygen fugacity is about 0.3 log units below the Ni-NiO buffer. Note that the order of volatility is Cd>Ag>Cu>In>Zn, in marked contrast to the anticipated relative volatilities from the condensation temperatures of Figure 1. Error bars 1 SD.

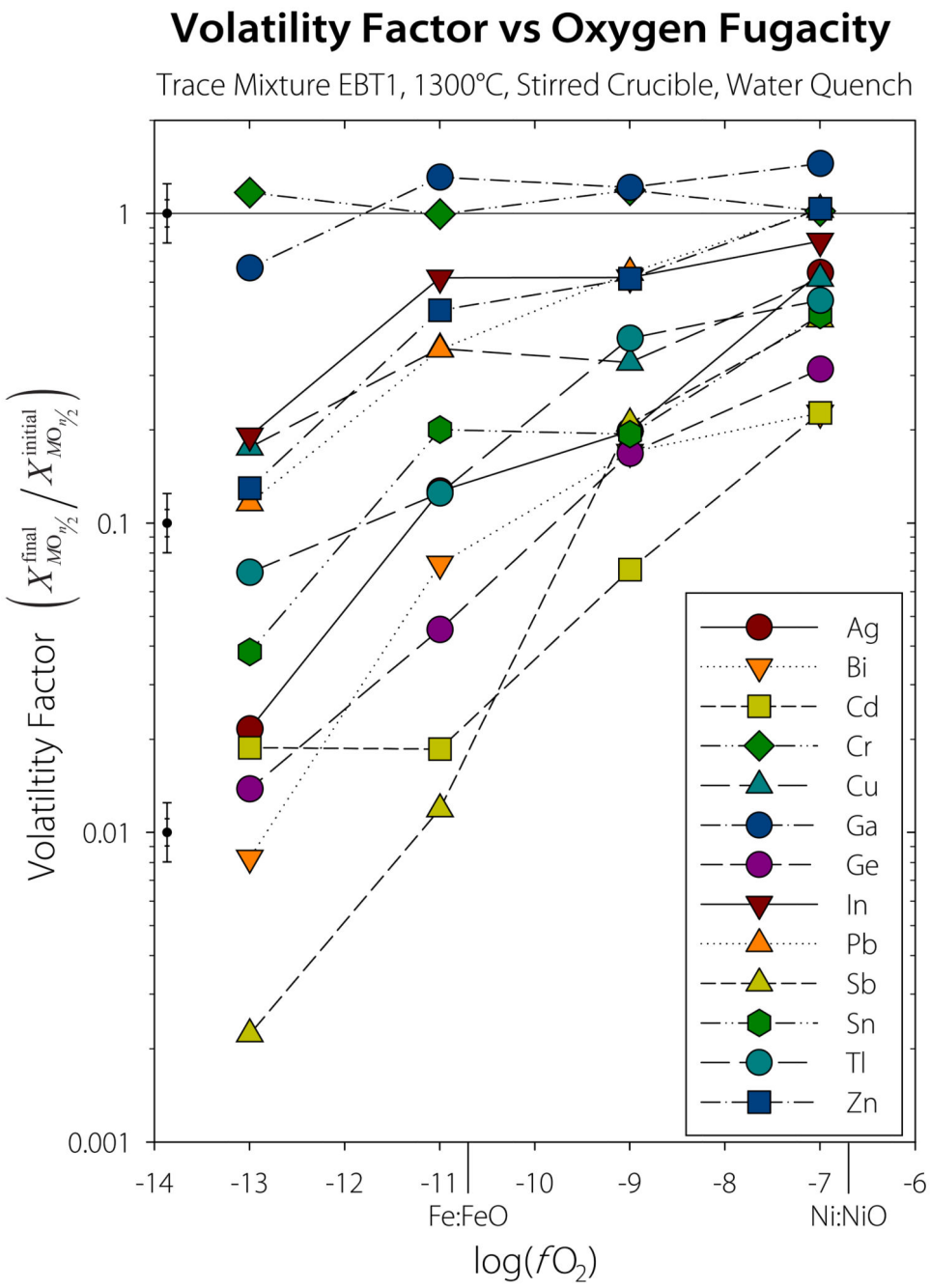

Figure 3.

This shows volatility factors as a function of oxygen fugacity for the elements we investigated at 1300°C. Volatility factors were calculated from the ratios of initial to final concentrations of the elements of interest after 60 minutes reaction in the constantly stirred melt. Indicative error bars of ±10% and ±20% are greater than 1 SD for virtually all elements and conditions (see text)

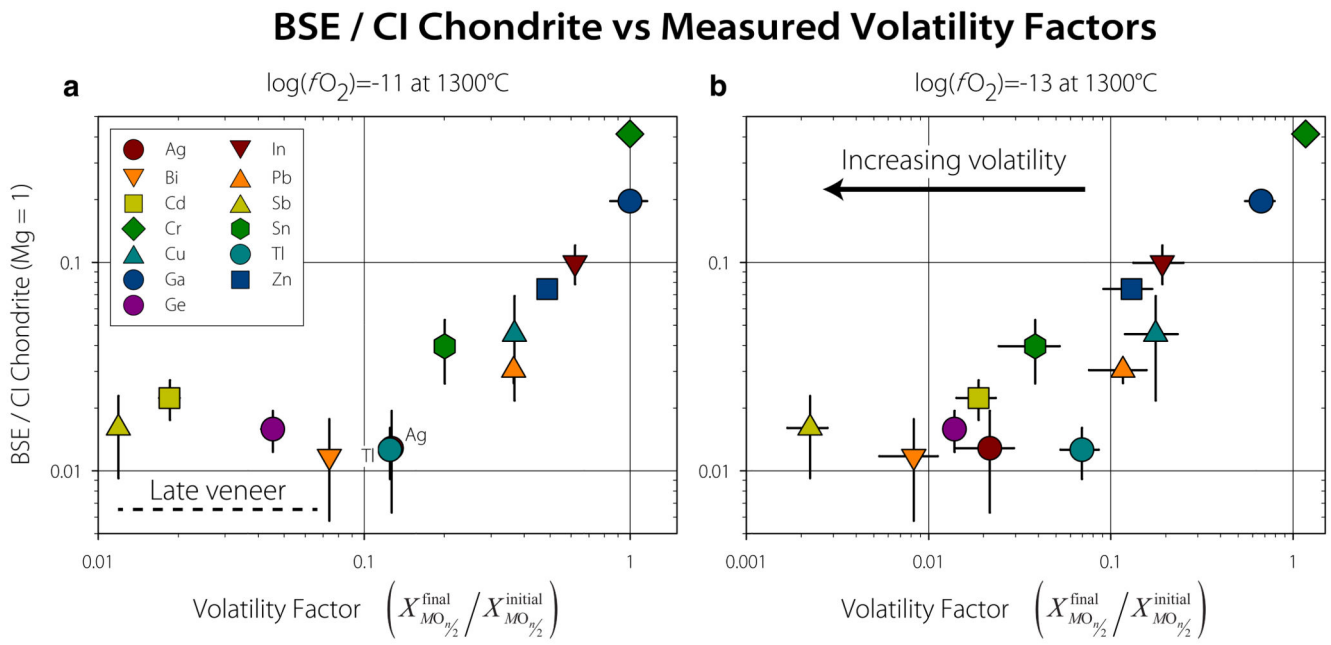

Figure 4.

a,b. This shows concentrations in Bulk Silicate Earth plotted as a function of measured volatility factors at log fO_2 of -11 and -13 at 1300°C. Concentrations of elements studied here are given relative to concentrations in CI chondrite meteorites1 (normalised to a concentration ratio of Mg of 1.0). Vertical error bars as in Figure 1. Horizontal error bars are 2 std errors. Line labelled “late veneer” refers to region where late addition of ~0.5% of chondritic material may have raised concentrations of the most volatile elements.

Europe PMC Funders Author Manuscripts